CHAPTER IV
RESULTS AND DISCUSSION

4.1 Analcime Dissolution in HCl

4.1.1 Dissolution Rate of Analcime in HCl

The rate of analcime dissolution was studied by digesting 0.5 g of analcime in 150 mL of HCl solution. The solution was stirred by magnetic stirrer at the stirring rate of approximately 500 rpm for all experiment. The variables studied were temperature (5 °C, 10 °C and 25 °C) and acid concentration (0.10 M-8.00 M).

The rate of dissolution of aluminum and silicon were calculated from the slopes of linear fitting to the initial aluminum and silicon dissolved versus time during the early stage of the experiment for various acid concentrations (Figure 4.1). Theoretically, the initial dissolution graph should pass the original point but my data did not. There are two possible reasons for this result.

Firstly, I did not treat my analcime sample before dissolving in the acid solution so that, my system still had the analcime particle <0.2 μm that can pass the filter.

The other is from my experimental error. If I push the stop watch after the actual starting time, the graphs will shift to the right hand site and will not pass the original point.

In the analcime structure, the covalent bonds between Si-O and Al-O are much stronger than ionic bonds between cation (Na^+) and the lattice network. After leaching of the surface, cation (Na^+) has been primary removed, thus, the network in the surface of the analcime will, then, contain the following groupings: Si-O-Si and Si-O-Al. When the network is being dissolved by the hydrochloric acid, these bonds must be broken for release of aluminum and silicon into the solution.

Table 4.1 shows that the ratio of the rate of silicon dissolution over the rate of aluminum dissolution. The results showed that the ratio were lower than stoicimetric ratio (2.25) at all concentration. These results can be explained by aluminum atom are selectively removal (Hartman *et al.*, 2005; Kerr, 1968).

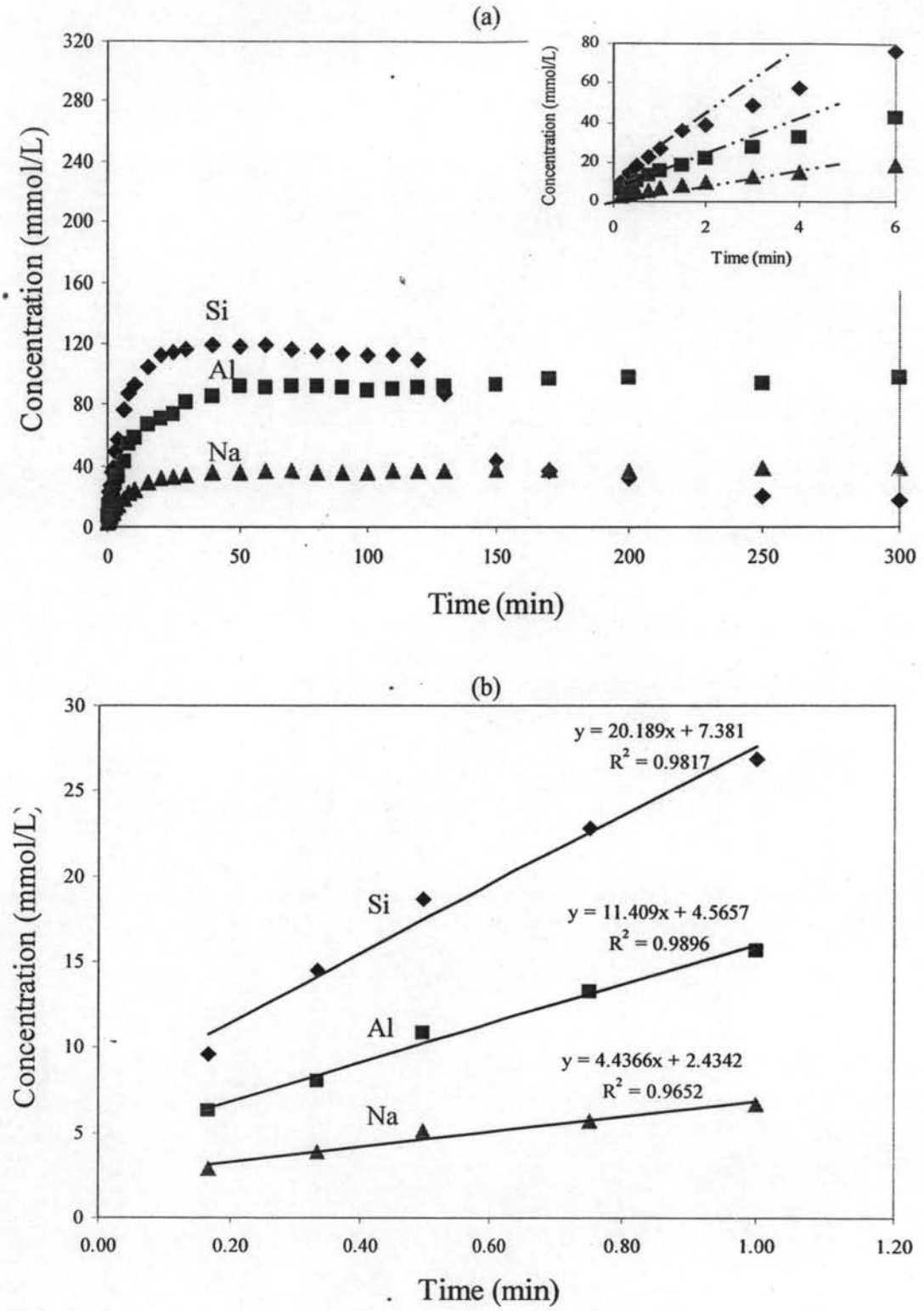

Figure 4.1 Rate data for typical dissolution experiment (a) dissolution curve of analcime in 8 M HCl at 5°C (b) initial dissolution rate method.

Table 4.1 The dissolution rate of aluminum and silicon of analcime in hydrochloric at 5 °C, 10 °C and 25 °C

Temperature	HCl concentration (mol/L)	$-r_{Si}$ (mmol/g.min)	$-r_{Al}$ (mmol/g.min)	$-r_{Si}/-r_{Al}$
5 °C	0.10	0.05	0.03	1.75
	0.25	0.10	0.06	1.81
	0.50	0.19	0.11	1.78
	1.00	0.35	0.19	1.87
	2.00	0.49	0.25	1.92
	4.00	0.62	0.34	1.82
	6.00	0.73	0.40	1.82
	8.00	0.77	0.42	1.83
10 °C	0.10	0.08	0.05	1.72
	0.25	0.16	0.08	1.99
	0.50	0.34	0.17	2.00
	1.00	0.46	0.25	1.82
	2.00	0.71	0.37	1.93
	4.00	0.94	0.49	1.90
	6.00	1.04	0.56	1.85
	8.00	1.08	0.58	1.86
25 °C	0.10	0.26	0.14	1.90
	0.25	0.50	0.27	1.85
	0.50	1.02	0.54	1.91
	1.00	1.79	0.94	1.90
	2.00	2.06	1.25	1.65
	4.00	2.62	1.50	1.74
	6.00	2.95	1.60	1.84
	8.00	3.00	1.75	1.72

Figure 4.2 shows the dissolution rate of aluminum and silicon for analcime as a function of H^+ concentration at 5 °C, 10 °C and 25 °C. The dissolution rate of aluminum and silicon increase with increasing the HCl concentration at all temperature. One can observe from Figure 4.2 that the apparent reaction order with respect to the H^+ concentration is approximately 1 at low concntration (<1.0 mol/dm^3) and decreases with increasing concentration as silicon and aluminum dissolution rates approach the plateau. A plateau of this type can be explained by an adsorption step in the reaction mechanism (Hartman *et al.*, 2005).

One of the suggested models by Hartman *et al.* (2005) is Langmuir-Hinshelwood rate law analogous to the Michaelis-Menten model. The mechanism is involving adsorption of the hydrogen ion followed by a surface reaction, which is rate limiting step. To test the suggested mechanism, the experimental data is linearized by the Hanes-Woolf method and shown in Figure 4.3.

Adsorption $H^+ + S \xrightarrow{k_1} H^+ \bullet S$

$H^+ \bullet S \xrightarrow{k_2} H^+ + S$

Surface Reaction $H^+ \bullet S \xrightarrow{k_3} products$ RLS

$$-r_{i,0}^{\bullet} = \frac{k_1 k_3 S_T [H^+]}{k_2 + k_3 + k_1 [H^+]} = \frac{k_3 S_T}{\frac{k_2 + k_3}{k_1} + [H^+]} = \frac{V_{\max,i}[H^+]}{K_{m,i} + [H^+]} \quad (4.1)$$

The kinetic dissolution parameters were determined for each temperature after linearizing and shown in Table 4.2.

Table 4.2 Evaluation of the kinetic parameters

Temperatue (°C)	**$V_{max,Si}$ (mmol/g.min)**	**$V_{max,Al}$ (mmol/g.min)**	**$K_{m,Si}$ (mol/L)**	**$K_{m,Al}$ (mol/L)**
5	0.94	0.52	1.88	1.89
10	1.31	0.71	1.64	1.70
25	3.51	2.03	1.27	1.38

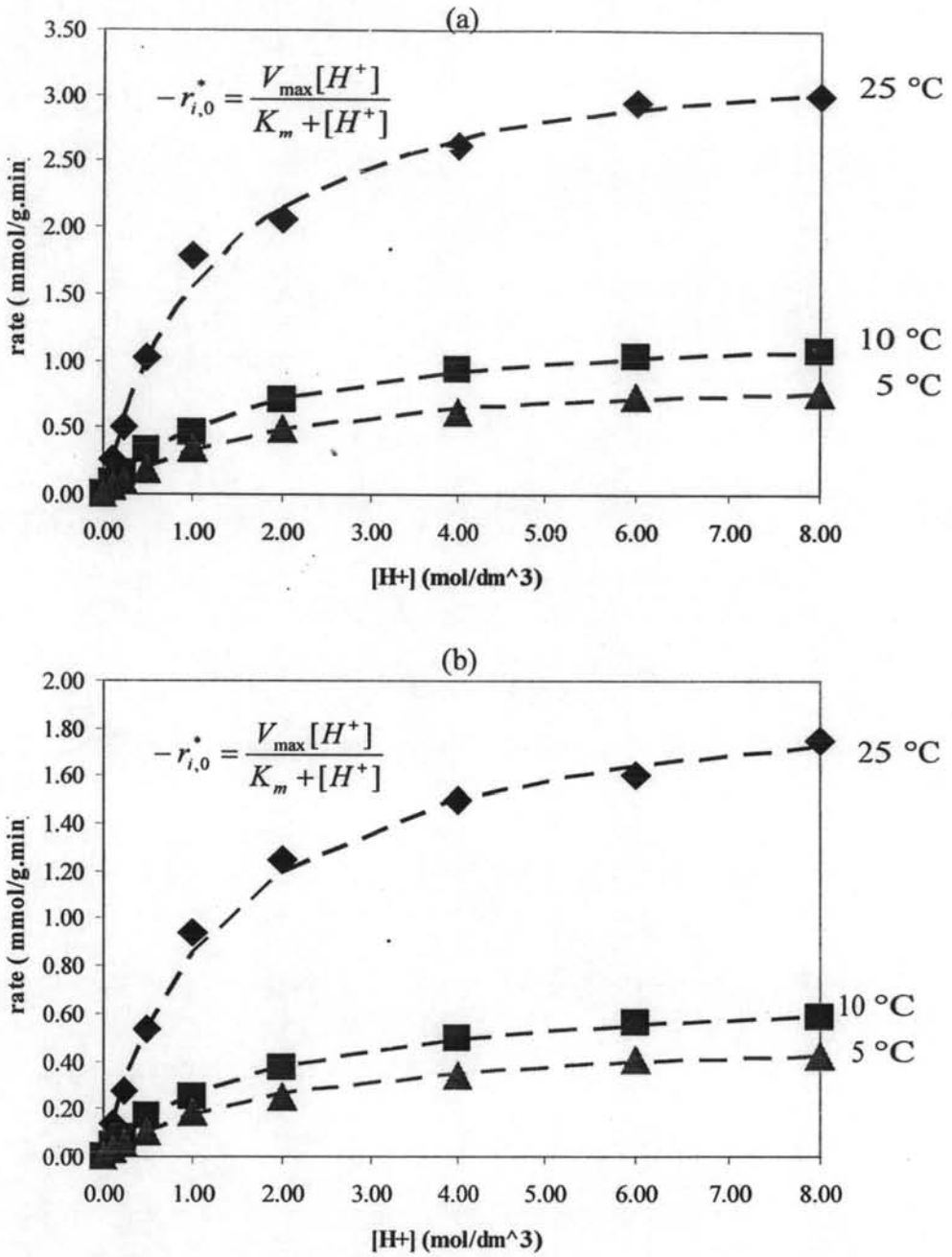

Figure 4.2 Analcime dissolution rate as a function of hydrogen ion concentration at 5 °C, 10 °C and 25 °C (a) Silicon (b) Aluminum.

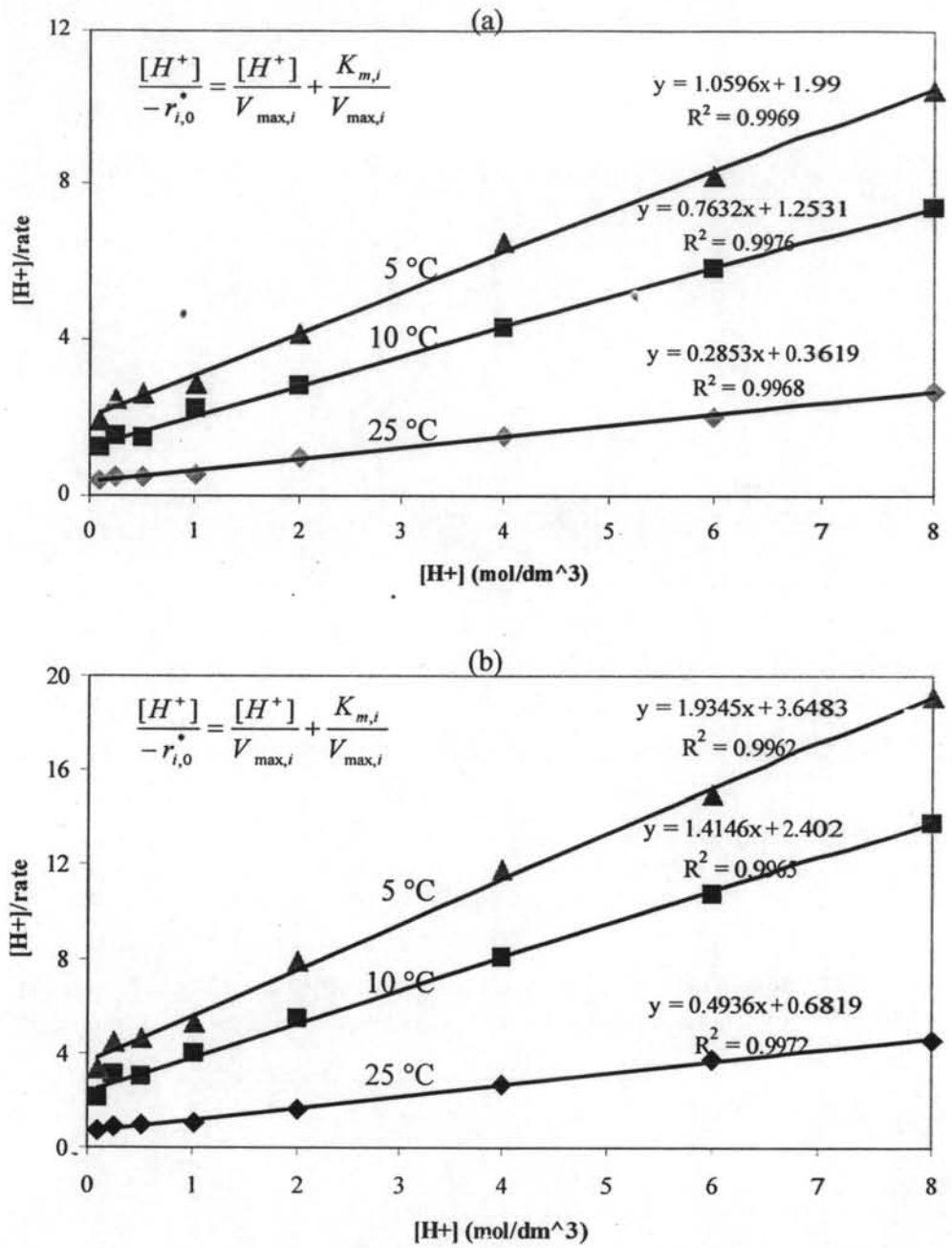

Figure 4.3 Hanes-Woolf plot for analcime dissolution at 5 °C, 10 °C and 25 °C (a) Silicon (b) Aluminum.

4.1.2 Activation Energy of The Reaction

The effect of temperature on rates of analcime dissolution in hydrochloric acid was investigated by performing the experiments at different temperatures. The experiments were conducted at 5 °C, 10 °C and 25 °C. The rates of dissolution of aluminum and silicon are shown in Table 4.2. The results indicated that the dissolution rates of both aluminum and silicon at higher temperature are faster.

The maximum rate of dissolution (V_{max}) at different temperature from Table 4.2 was used to determination of the activation energy of the dissolution. The quantitative relationship for the activation energy is given by the Arrenius equation:

$$k = A\exp(-E_a/RT) \qquad (4.2)$$

where k = specific surface reaction rate constant (mmol/(g.min.HCl molarity))

A = frequency factor or pre-exponential factor

E_a = activation energy (J/mol)

R = gas constant = 8.314 J/mol.K

T = absolute temperature (K)

From Arehenius equation, activation energy can be found by plotting ln (V_{max}) as a function of 1/T . The plot was shown in Figure 4.4.

The activation energy of the surface reaction for the dissolution of aluminum from analcime in HCl is approximately 47.38 kJ/mol and the activation energy of the surface reaction for the dissolution of silicon from analcime in HCl is approximately 45.52 kJ/mol.

The activation energy results from my experiment agree with Wilkin *et al.* (2001) who studied the effect of temperature and free energy of analcime precipitation and dissolution rates at temperature 125 and 175 °C. Their activation energy value is 10.9 $\pm$ 1.7 kcal/mol.

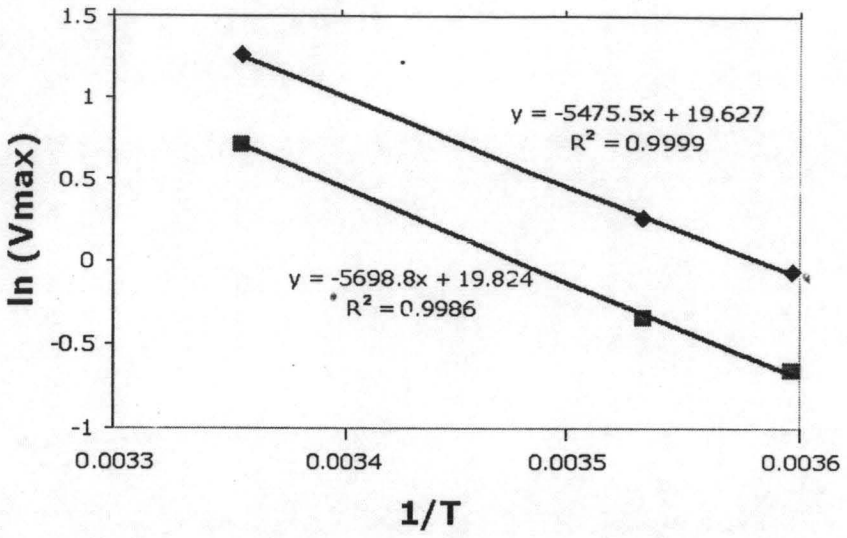

Figure 4.4 Plot of 1/T vs $\ln(V_{max})$ for finding activation energy.

4.2 Analcime Dissolution in Citric Acid

4.2.1 Dissolution Rate of Analcime in Citric Acid

The rate of analcime dissolution was studied by digesting analcime in citric acid solution. The solution was stirred by magnetic stirrer at the stirring rate of approximately 500 rpm for all experiment. The variables studied were acid concentration (0.25 M-3.00 M) and temperature (5 °C and 25 °C). The dissolution curves of aluminum and silicon from analcime are shown in Figure 4.5.

The rate of dissolution of aluminum and silicon were calculated from the slopes of linear fitting to the initial aluminum and silicon dissolved versus time during the early stage of the experiment for various acid concentrations. Figure 4.6 shows the dissolution rate of aluminum and silicon for analcime in citric acid as a function of citric acid concentration at 5°C. The dissolution rate increased with increasing citric acid concentration. This phenomenon is the same as the analcime dissolution in hydrochloric acid so that the Michelis-Menten model was applied to this result as well. The kinetic parameters were calculated and shown in the Figure 4.6.

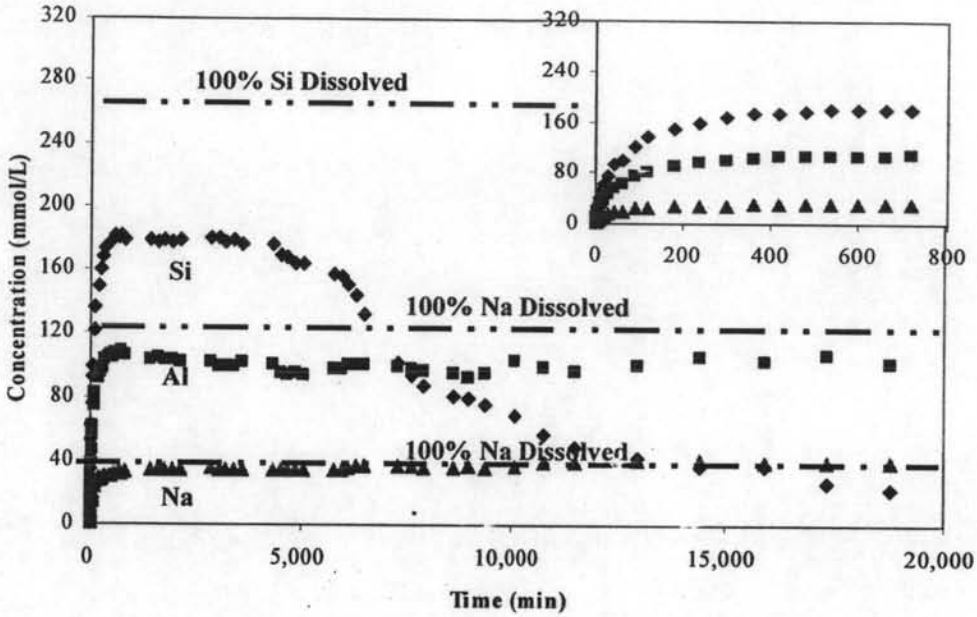

Figure 4.5 The dissolution curves of silicon, aluminum and sodium from analcime in 3.00 M citric acid.

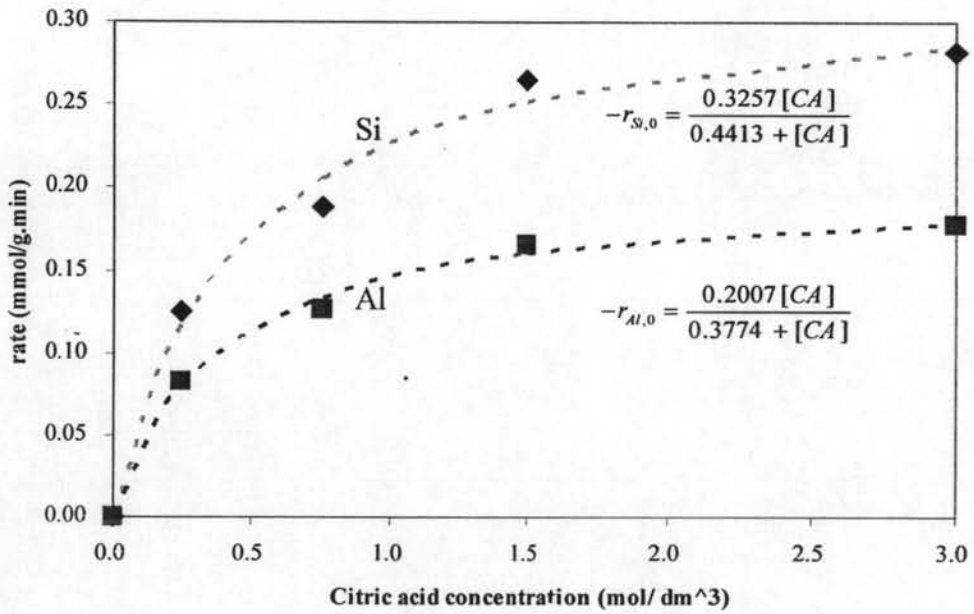

Figure 4.6 The dissolution rate of analcime as a function of citric acid concentration at 5 °C.

4.2.2 The Change of Surface Morphology and Composition during Dissolution

Un-dissolved analcime particles in 3 M citric acid at 5 °C were collected via filtration at different reaction times. The surface morphology was observed under Scanning Electron Microscope (SEM) as shown in Figure 4.7. The compositions in the surface were analyzed by Energy Dispersive X-ray Spectroscopy (EDX). The surface composition was found to be different at the different time as shown in Figure 4.8. At time less than 10 min, the particles appeared to be un-reacted as can be seen in Figure 4.7 (b) and 4.7 (c). After 25 min in the acid, etched pits and channels were noted on the particle surface in Figure 4.7 (d), and by 50 min the etched pits and channels had grown as can be seen in Figure 4.7 (e). Figure 4.7 (f) demonstrates that the structural integrity of the particles had been lost after 100 min. The broken particles remained un-dissolved at 400 and 2000 as shown in Figure 4.7 (h) and 4.7 (i). At 4500 min and thereafter, the un-dissolved particles coexisted with a newly formed precipitate phase as can be seen in Figure 4.7 (j), (k) and (l).

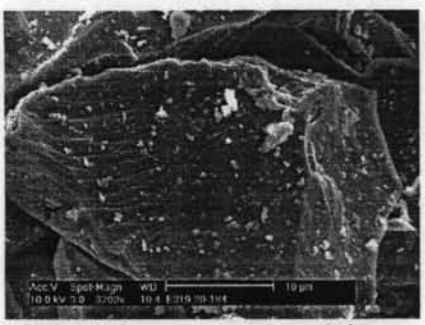

(a) Initial un-reacted analcime

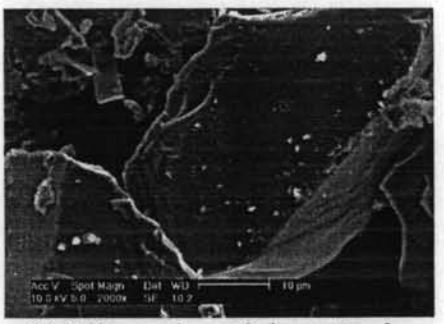

(b) Filtrated particle at 5 min

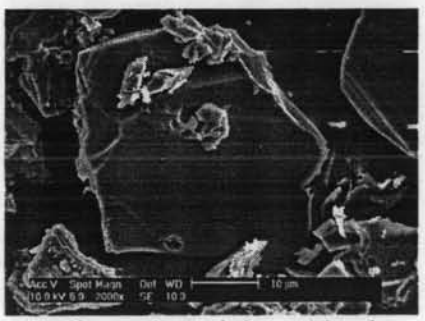

(c) Filtrated particle at 10 min

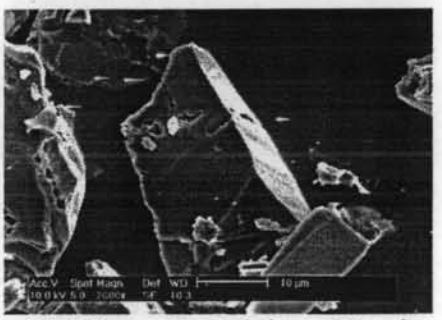

(d) Filtrated particle at 25 min

(e) Filtrated particle at 50 min

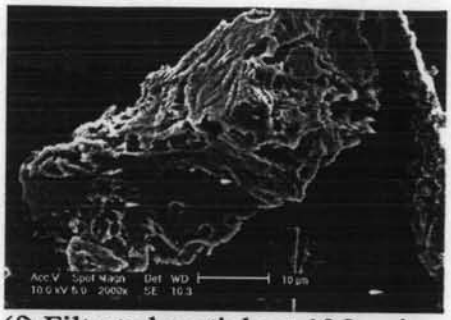

(f) Filtrated particle at 100 min

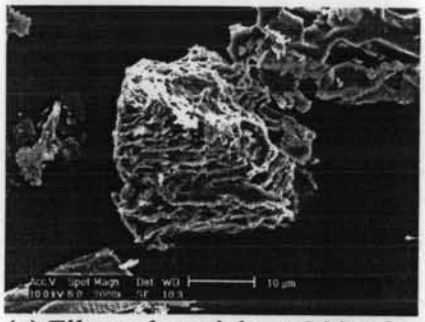

(g) Filtrated particle at 200 min

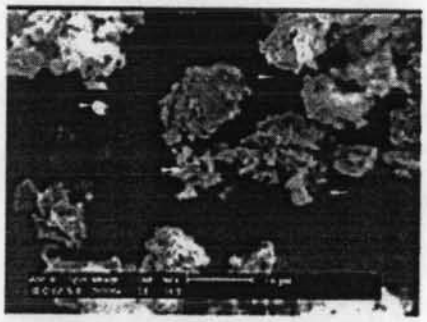

(h) Filtrated particle at 400 min

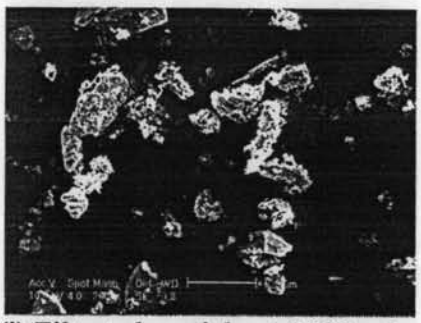

(i) Filtrated particle at 2000 min

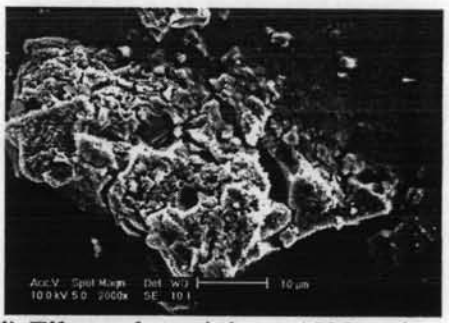

(j) Filtrated particle at 4500 min

(k) Filtrated particle at 10000 min

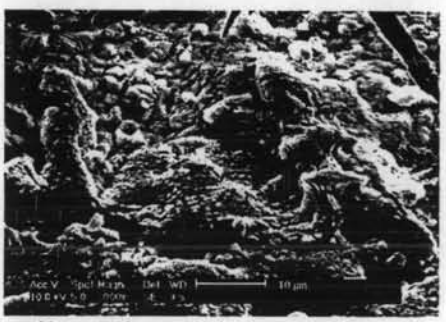

(l) Filtrated particle at 20000 min

Figure 4.7 Scanning electron micrographs of dissolving analcime particles at different reaction time.

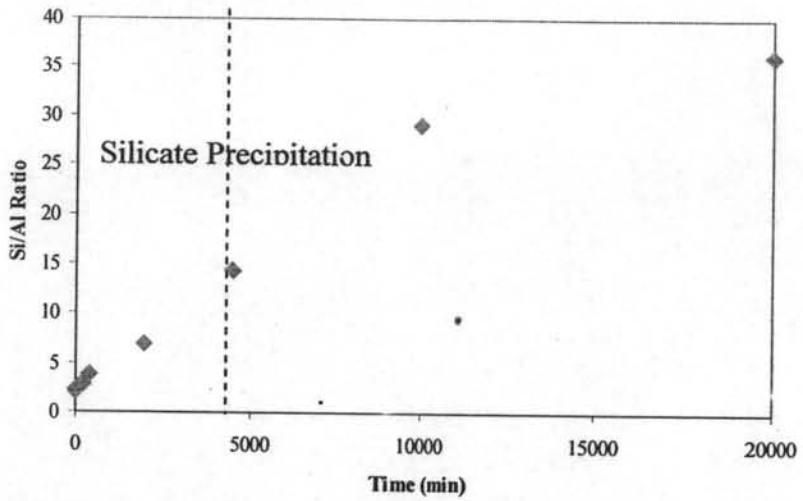

Figure 4.8 Silicon to Aluminum ratio of the un-dissolve particles.

4.3 Comparison Initial Dissolution of Analcime in HCl and Citric Acid

4.3.1 Dissolution Rate of Analcime in Mixture of Citric acid and Hydrochloric Acid

Figures 4.9 and 4.10 show that the attack of analcime by citate ion is negligible compared to the rate of dissolution in citric acid.

At pH value less than one, virtually all of the citric acid present in the solution of hydrochloric is in the form of molecular citric acid, consequently, further increases in the concentration of citric acid ion do not change the concentration hydrogen ion, although the rate of dissolution can be increased substantially. Since the enhanced rate of analcime dissolution when citric acid are present cannot be attributed to changes in the identity or the concentration of the hydrogen ion, the exciting conclusion is that the observed increases result from a catalytic process at the solid liquid interface.

The overall dissolution in this case should result from parallel catalyzed and uncatlyzed reactions.

The degree of acid catalysis, D_{AC}, is defined as the fraction by which the overall rate of dissolution, -r is greater than the uncatalyzed reference rate, $-r_0$,

$$D_{AC} = \frac{r}{r_0} - 1 \qquad (4.3)$$

The degree catalysis for the dissolution of analcime in mixture of 0.5 M hydrochloric and citric acid at 25 °C was shown in Figure 4.11.

Another important result of this investigation is that the degree of catalysis is not an unbounded function of the bulk concentration of the citric acid concentration. Rather, the catalysis of the dissolution of analcime is limited by a specific maximum value. In the context of a surface reaction, the asymptotic nature of Figure 4.11 constitutes further evidence of equilibrium between citric acid in the bulk and unoccupied catalysis sites, where the asymptote represents the limit of total surface coverage.

The experimental evidence indicates that the overall dissolution consist of parallel catalyzed and uncatalyzed reactions. The nature of the uncatalyzed reaction and characteristic rate laws have been discussed previously. The adsorption of hydrogen ion followed by a surface reaction is represented by the following equation

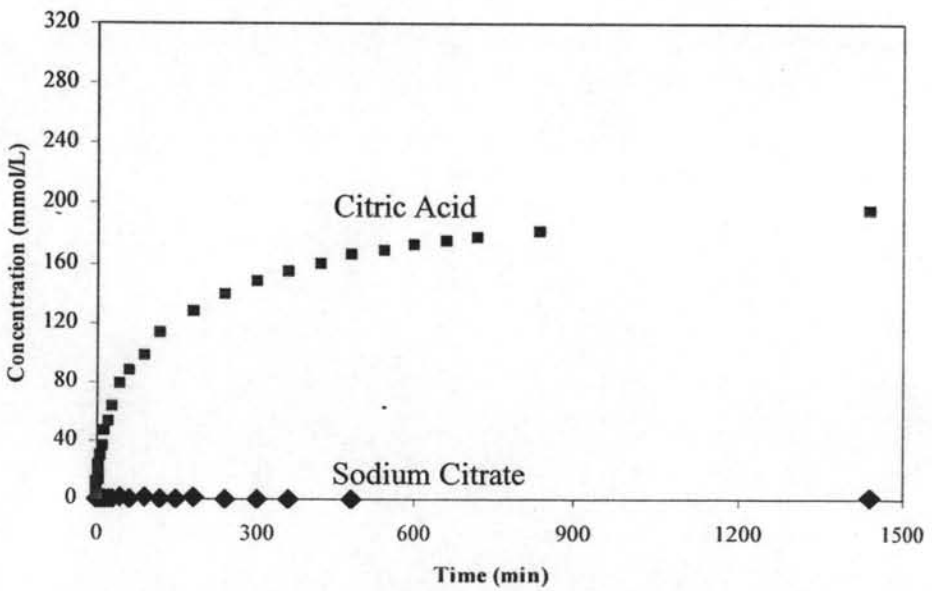

Figure 4.9 Analcime dissolution in 1.5 M citric acid and in 1.5 M sodium citrate at 5 °C (Silicon).

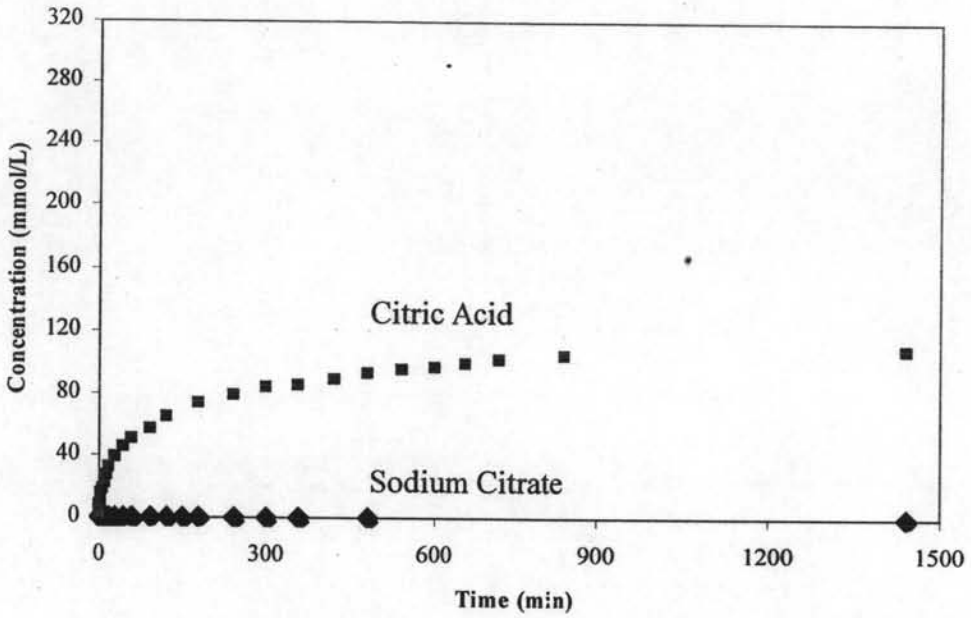

Figure 4.10 Analcime dissolution in 1.5 M citric acid and in 1.5 M sodium citrate at 5 °C (Aluminum).

$$H^+ + S' \Leftrightarrow H^+ \bullet S'$$

$$H^+ \bullet S' \rightarrow Products$$

$$-r_{uncatalyzed} = k' C_{H^+ \bullet S} = \frac{k' K_A [H^+] C_{T'}}{1 + K_A [H^+]} \qquad (4.4)$$

Where

H^+ = the bulk concentration of hydrogen ion

$C_{H^+ \bullet S}$ = the concentration of the sites occupied by adsorbed hydrogen ion

C_T = the total concentration of sites that can be occupied

K_A = the equilibrium adsorption constant

k' = the specific rate constant for the uncatalyzed reaction

The catalyzed reaction, on the other hand, is a function of the surface concentration of both hydrogen ion and citric acid. If we assume the citric acid and hydrogen ion adsorb on the different sites the catalyzed reaction can be written as:

$$H^+ \bullet S + CA \bullet S' \rightarrow \text{Products}$$

Assuming a first order dependence with respect to both attacking hydrogen ion and the catalyzing citric acid, one can now write the following rate law for the catalyzed reaction

$$-r_{catalyzed} = k * C_{H^+ \bullet S} * C_{CA \bullet S} \tag{4.5}$$

or

$$-r_{catalyzed} = \frac{kC_T \cdot C_T K_A [H^+]}{1 + K_A [H^+]} \frac{K_B [CA]}{1 + K_B [CA]} \tag{4.6}$$

Combining constants and adding equation 4.4 and 4.6 for the uncatalyzed and catalyzed reactions gives an expression for the overall rate of dissolution.

$$-r = \frac{k_0 K_A [H^+]}{1 + K_A [H^+]} (1 + \frac{k_1}{k_0} \frac{K_B [CA]}{1 + K_B [CA]}) \tag{4.7}$$

One notes that the first term of the right hand side of equation 4.7 is $-r_0$. Consequently the fraction by which the dissolution is catalyzed by the presence of citric acid it the bulk solution, D_{AC}, can be

$$D_{AC} = \frac{r}{r_0} - 1 = \frac{k_1}{k_0} \frac{K_B [CA]}{1 + K_B [CA]} \tag{4.8}$$

The validity of the Langmuir isoterm used in the model can be test by plotting $1/D_{AC}$ as a function of 1/[CA] as shown in Figure 4.12, linear relationships were obtained over the entire concentration range.

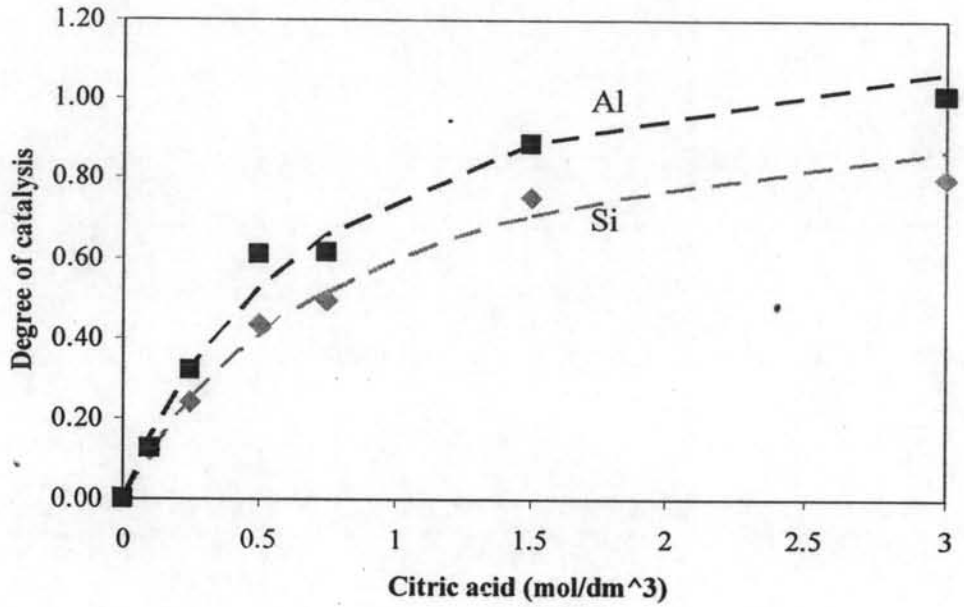

Figure 4.11 Degree of catalysis of citric of citric acid in 0.5 M hydrochloric acid.

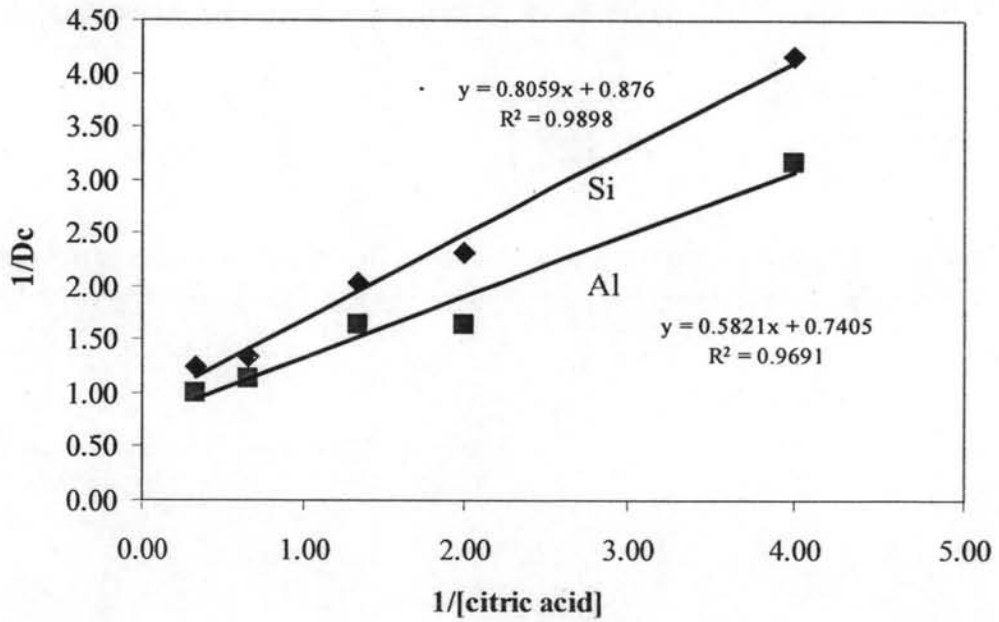

Figure 4.12 Plot of $1/D_{AC}$ as a function of 1/[CA].

4.3.2 Citric acid – Analcime Interactions

Figure 4.13 shows the dissolution rate of aluminum and silicon compared between in HCl and in citric acid at the same hydrogen ion concentration. The results indicate that the dissolution rate of both silicon and aluminum in citric acid are much faster than in HCl at the same hydrogen ion concentration that might be a catalytic process at the solid liquid interface. It was found that citric acid has more catalytic effect on aluminum than on silicon because citric acid might prefer to adsorbing on aluminum.

Soluble organic acids can affect the rate of mineral dissolution by at least three mechanisms. Though generally weak acids, these compounds produce protons, which attach to oxygen sites at the mineral surface, weakening the metal-oxygen bond and catalyzing the dissolution reaction. The rate of dissolution by this proton-promoted mechanism is controlled by the rate of hydrolysis at the mineral surface. (Susan *et al.,* 1992).

Soluble organic acids can also complex metal ions in solution, thus increasing the apparent solubility of the mineral. This process may indirectly increase the mineral dissolution rate, particularly if the solution is close to equilibrium with respect to the dissolving solid (Bennett *et al.,* 1988). In the case of analcime, the formation of Al- and possibly Si-organic complexes in solution (Bennett *et al.,* 1988; Bennett *et al.,* 1991) can shift the equilibrium toward increased apparent mineral solubility, thus increasing the analcime dissolution rate. If solution concentrations are kept far from equilibrium saturation with respect to the dissolving phase, where dissolution rates are apparently zero-order with respect to solution concentration, this process should have no impact on overall dissolution rates.

Aluminum is presumed to be complexed primarily by difunctional organic acids via a bidentate chelate, forming a ring structure that incorporates two Al-O-C bonds. Five- member rings were found to be most stable, such as the oxalate complexes of aluminum, while four- or six-member rings were less so. Catechol complexes of aluminum have also been characterized, using UV-difference methods, and were found to consist of I: 1 and 2: 1 complexes (Sikora and McBride, 1989).

The role of organic acids in complexing silica in natural waters, however, is not well documented. Silica-organic complexes with Si-C and Si-O-C linkages are well characterized only in non-aqueous systems though the existence of Si -0-C ester-bonded complexes is recognized in biochemical and some aqueous systems (Iler, 1979). Hydrogen-bonded complexes involving an ≡Si-0-H•••0-C-R linkage are also thought to occur in aqueous systems and on silica surfaces (Iler 1977). Iler (1979) *describes the chemistry of a silica-catecholate complex, and suggests that a 1:3 complex forms, with the silicon metal center coordinated with three catechol ligands in an octahedralgeometry. Similar findings have been reported for other silicon-organic complexes.

Metal-organic complexes can also form at the solid-solution interface, thereby weakening the cation-oxygen bond and thus catalyzing the dissolution reaction (ligand-promoted dissolution) (Kummert and Stumm, 1980; Stumm *et al.*, 1980).

This interaction may be strong enough to decrease the energy needed to break framework bonds, resulting in an increased rate of dissolution accompanied by decrease activation energy. It may also increase the rate of decomposition of the transition state complex, or may weaken framework Si-0-Si bonds. Or it may alter the geometry of the HO-X bond, thus decreasing the steric hindrance encountered by hydrogen ion molecules during the dissolution reaction of analcime.

Organic acids contribute significantly to mineral dissolution, where the effect of proton- promoted dissolution is smallest. The degree of catalysis by organic acid ligand decreases as pH decreasing. This result indicates that proton-promotes dissolution becomes relatively more important at higher acidities.

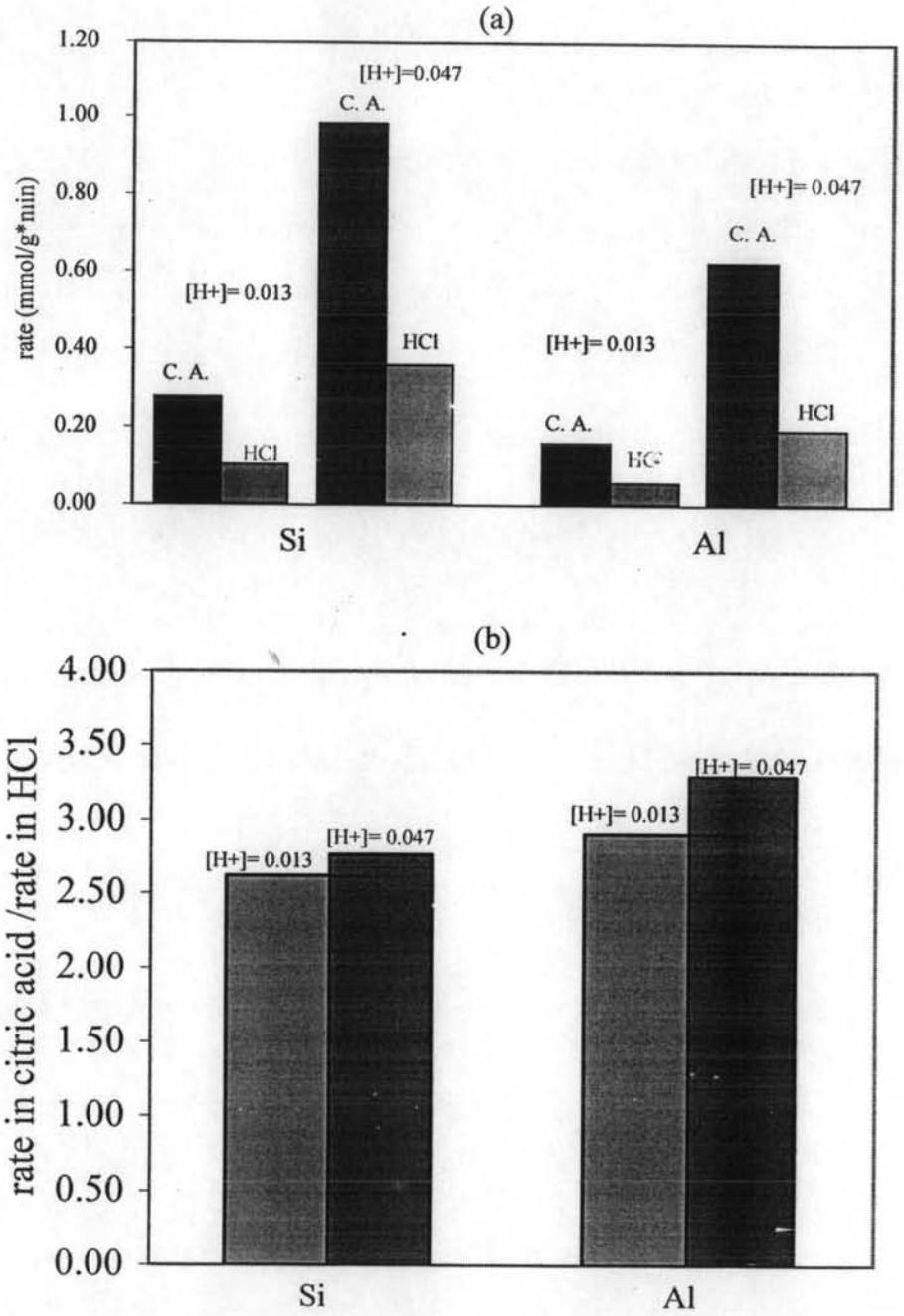

Figure 4.13 Dissolution rate of analcime compared between in HCl and in citric acid at the same [H+] (a) dissolution rate (b) $r_{Citric\ acid}/r_{HCl}$.

4.4 Silicate Precipitation

4.4.1 Silicate Precipitation in HCl

Figure 4.14 shows the concentration profiles of aluminum and silicon in the solution as the function of time from analcime dissolution in 8 M HCl solution at 25 °C. The curve of silicon and aluminum in the solution increase until it reach the plateau. A plateau of this type can be explained by the selectively removal of aluminum. After all of aluminum removed the dissolution stopped (Hartnan *et al.*, 2005). After that, the concentration of silicon slowly decreased and then remained constant. The result indicated that some silicon dissolve in HCl solution precipitated out. As dissolution progressed, the solution became saturated with monosilicic acid. Subsequent silicate dissolved from the zeolite matrix then precipitates immediately from solution as amorphous silicate in the form of a white pasty gel as observed in the experiment.

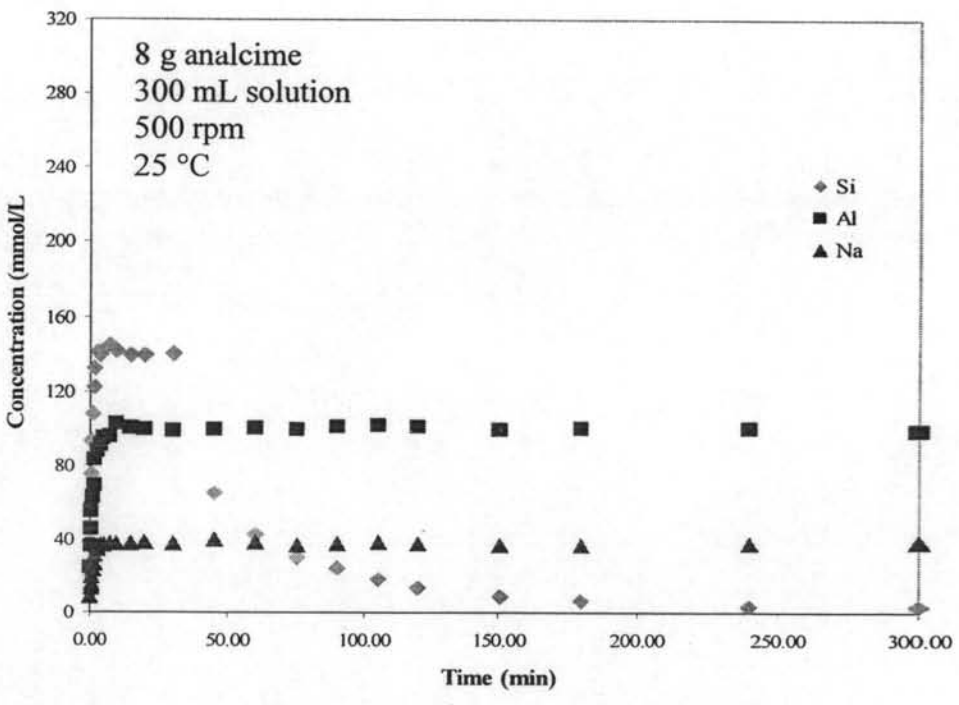

Figure 4.14 Concentration profiles of aluminum and silicon from analcime dissolution in 8 M HCl at 25 °C.

4.4.2 Silicate Precipitation in Citric Acid

Silicate precipitation was studied by dissolving analcime in 300 ml of citric acid. The solution was stirred by magnetic stirrer at the stirring of approximately 500 rpm for all experiment. The variables studied were concentration of citric acid, amount of analcime and temperature.

The effect of citric acid concentration on the silicate precipitation was shown in Figure 4.15. It was found that the higher the citric acid concentration the faster precipitation rate.

The effect of amount of analcime on the silicate precipitation in 3.00 M citric acid was shown in Figure 4.16. It was found that the lower amount of analcime the longer induction time and slower precipitation rate.

Figure 4.17 shows the silicon concentration profile as a function of time in 3.00 M at 5 °C and 25 °C. The result show that increasing the temperature, the precipitation rate also increase.

The effect of citric acid concentration, amount of analcime and temperature can be further explained by normal nucleation theory. In order to nucleate a cluster of volume V and area S the energy required is

$$\Delta G = -\frac{V}{\Omega} k_B T \ln\beta + S\gamma \qquad (4.9)$$

Where

Ω = the volume of a molecule inside the crystal

γ = the interfacial free energy between nucleus and solution

k_b = Boltzmann constant ($1.38*10^{-23}$ m^2 kg s^{-2} K^{-1})

T = absolute temperature

Hence, the first term of equation 4.9 is a volume term, V/Ω being the number of molecules inside the nucleus. The second term, the surface term, represents the excess energy expended in the creating the nucleus surface. It is supposed here that γ has the same value over the whole nucleus surface, or that the nucleus is limited by crystallographically equivalent faces. If we consider a spherical nucleus equation 4.9 become

$$\Delta G = -(\frac{4\pi r^3}{3\Omega})k_B T \ln\beta + 4\pi r^2\gamma \qquad (4.10)$$

Due to the competition between volume and surface term, ΔG passes through a maximum at a certain value of r. In other words, when the nucleus reach the critical radius. The critical activation free energy for nucleation is

$$\Delta G^* = \frac{16\pi\Omega^2\gamma^2}{3(k_B T \ln\beta)^2} \qquad (4.11)$$

At the critical values, the nucleus is stable. If one molecule is withdrawn from it ($r<r^*$), it dissolves spontaneously. On the other hand, if one molecule is added to it($r>r^*$), it grows spontaneously, both process taking place with and energy gain.

Equation 4.11 shows that the activation free energy for nucleation decreases with increasing supersaturation ratio and temperature, and decreasing interfacial free energy. Nucleation rate for homogeneous nucleation is

$$J = K_0 \exp(-\Delta G^* / k_B T) \qquad (4.12)$$

where

K_0 = kinetic coefficient

ΔG^* = critical active free energy

We may expect a larger nucleation rate at high supersaturation ratio and temperature. When we increase the concentration of citric acid we decrease the solubility of monosilicic acid thus, resulted in increasing supersaturation ratio.

When increase the amount of analcime we also increase the monosilicic acid concentration in the solution that mean we increase supersaturation ratio as well so that, the precipitation rate is increased.

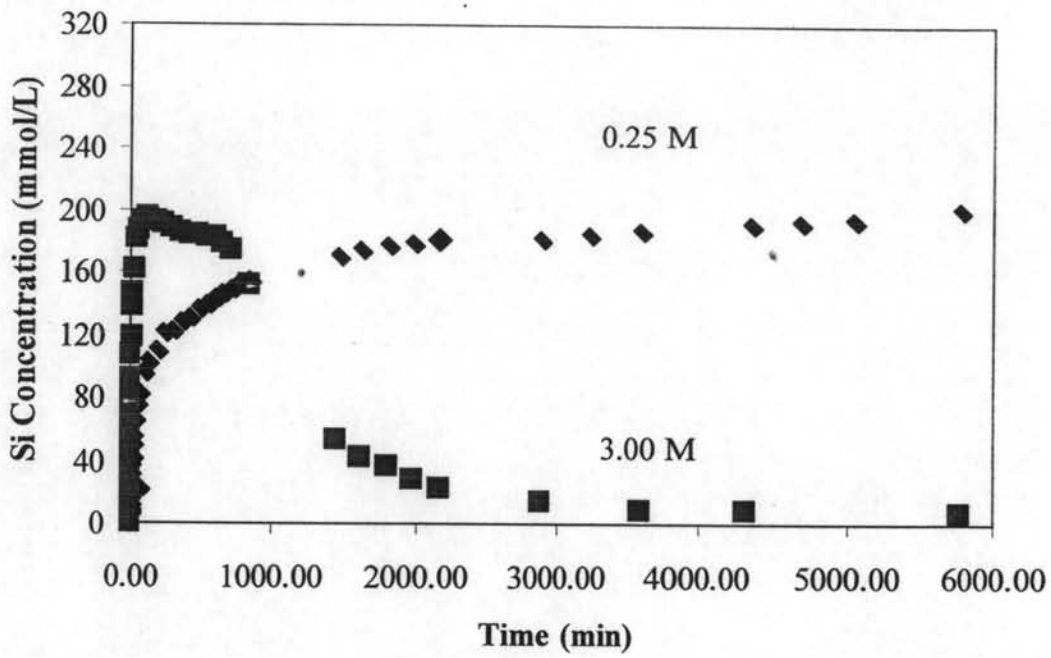

Figure 4.15 Effect of citric acid concentration on silicate precipitation.

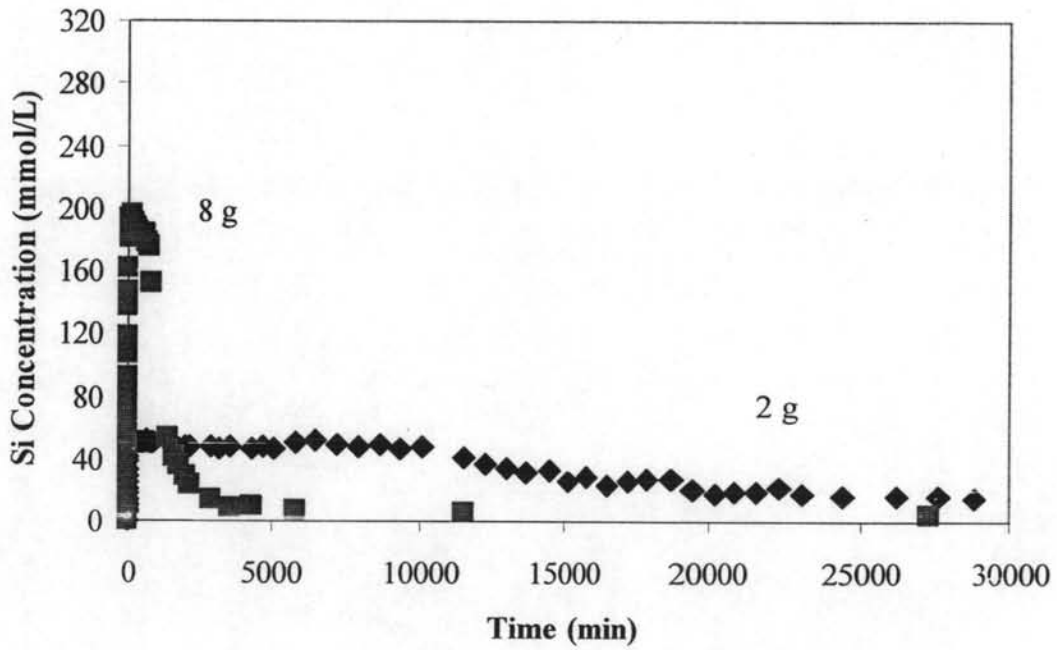

Figure 4.16 Effect of amount of analcime on silicate precipitation in 3 M citric acid.

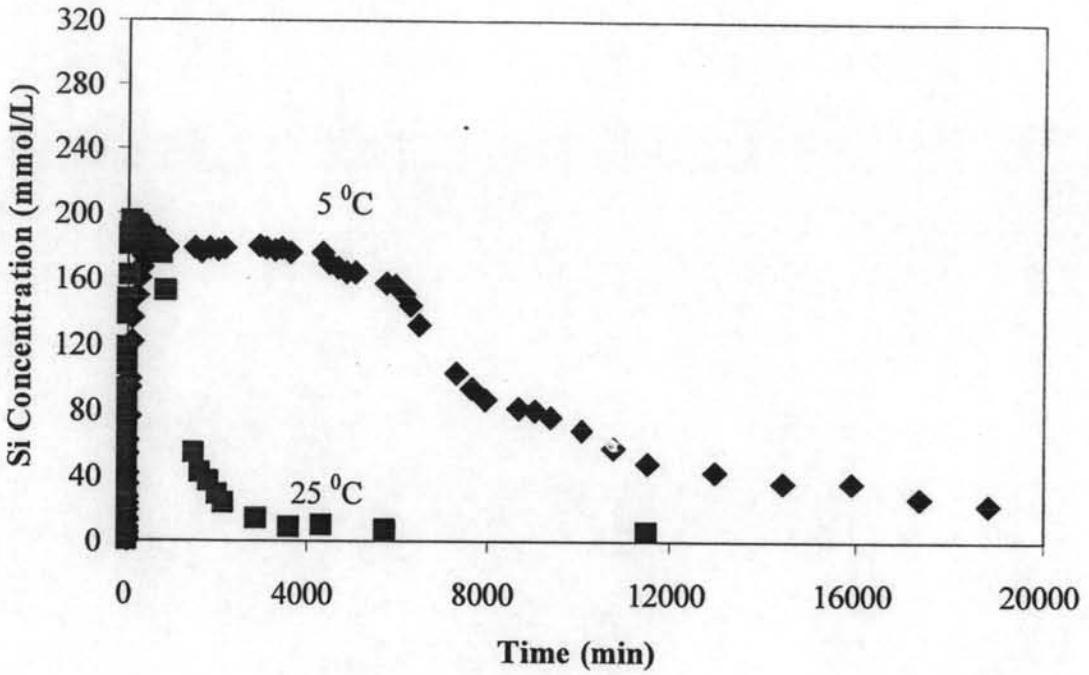

Figure 4.17 Effect of temperature on silicate precipitation in 3 M citric acid.

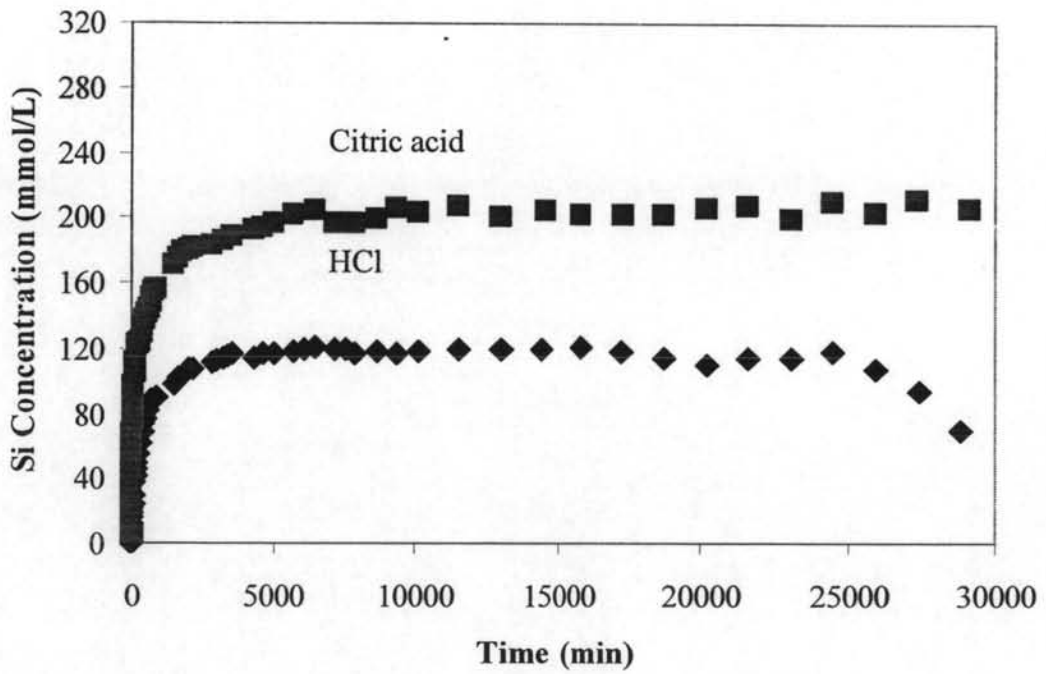

Figure 4.18 Comparison silicate precipitation in HCl with in citric acid at 25 ^{0}C ; pH 1.44.

4.4.3 Possible Inhibition Mechanism by Citric acid

In the presence of citric acid, silicate precipitation rate is slower that in HCl as shown in Figure 4.18. The nuclei of silicate particle are initially formed from the polymerization reaction between monosilicic acid. Afterwards, when the stable nuclei gradually growing in a supersaturated system become larger than the critical size, they start growing into crystal. However, in the presence of citric acid, the precipitation rate trend to decrease because citric acid plays an important role in lowering or completely preventing the formation and growth of silicate precipitate particle. Generally, there are two possible mechanisms to inhibit the silicate formation and growth.

1. Citric acid forms complex with monosilicic acid. The complex forms unable to form the nuclei. There are two possible complex forms of citric acid and monosilicic acid (bidentate forms and tricdentate form) as shown in Figure 4.19.

2. Citric acid adsorbs and cling to the active growth sites of the growing silicate. The adsorption can block the growth process of the silicate particles. Hence, the blockage of the particles results in no longer growing.

Another possible mechanism is that citric acid can form complex with aluminum, leading to a decrease in ionic strength, thus decreasing the supersaturation ratio.

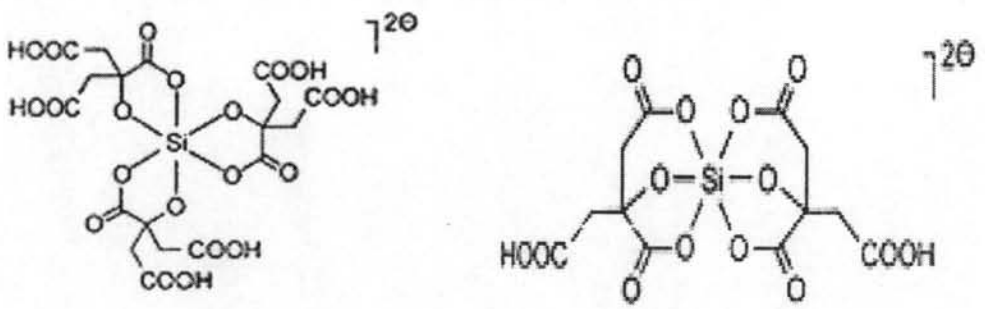

(a) (b)

Figure 4.19 Possible complex form between citric acid and monosilicic acid (a) bideiate form (b) tridentate form.